AALBORG UNIVERSITY

Three-Fold Symmetry Restrictions on Two-Dimensional Micropolar Materials

Warren, W. E.; Byskov, Esben

Link to publication from Aalborg University

Three-Fo

Three-Fold Symmetry Restrictions on Two-Dimensional Micropolar Materials

W.E. Warren, E. Byskov

Three-Fold Symmetry Restrictions on Two-Dimensional Micropolar Materials

W.E. Warren, E. Byskov

Three-Fold Symmetry Restrictions
on
Two-Dimensional Micropolar Materials

William E. Warren[a] and Esben Byskov[b]

[a]Department of Mechanical Engineering, University of New Mexico, Albuquerque, NM 87131, USA
[b]Department of Building Technology and Structural Engineering, Aalborg University, Sohngaardsholmsvej 57, DK-9000 Aalborg, Denmark

December 19, 2000

Abstract—Analysis of the mechanical properties of engineering materials with microstructure generally requires modification of the concept of a simple material. One approach is the theory of micropolar materials which introduces an independent rotation of a material element and the resulting stress and strain tensors are generally non-symmetric. In two-dimensional material models these microstructures are often represented by geometries which exhibit three-fold symmetry in the plane. In this work we investigate the form of the constitutive relations which this three-fold symmetry imposes. We show that three-fold symmetry requires both the stress and couple stress tensors to be isotropic in the plane. We obtain the constitutive relations for an equilateral triangle structure and for the hexagonal or honeycomb structure, both of which exhibit three-fold symmetry in the plane. These results are compared with the results of previous investigations of these two-dimensional material models.

1 Introduction

Many engineering materials display a pronounced microstructure which often must be taken into account in the analysis of their mechanical properties. These materials include low density cellular foams, wood, fiber reinforced polymers, granular media including cementitious materials, and numerous biological materials. A number of sophisticated averaging techniques have been developed to model these materials with microstructure as simple materials within the framework of classical continuum mechanics (Nemat-Nasser & Hori 1993). This continuum model of a simple material in which the stress at a material point depends only on the strain at that point, often referred to as "local" materials, has proven to be quite effective in representing the mechanical response of solid materials under most conditions. However, the nature of a discrete microstructure in some materials presents a significant problem in modeling these materials as continua in certain situations. This limitation of the classical theories has been pointed out by Koiter (1964) among others. Of particular

concern are those situations in which severe deformation occurs within highly localized regions of the material where the size scale of the deformation region is of the same order as that of the microstructure.

An alternative to the simple continuum model is the micropolar material model developed by Eringen & Suhubi (1964). In this model, a material point within the body undergoes the usual displacement from its original position, and in addition, the material point is assumed to undergo a rotation which is independent of the displacement. This model obviously encounters severe philosophical difficulties if considered as representative of a continuum. It does, however, reflect the mechanics of a discrete structure where, for example, the forces and moments in a beam connecting two masses require information about the relative rotations as well as the displacements of the two masses. Several researchers have modeled structural frameworks as micropolar continuum (Askar & Cakmak 1968, Sun & Yang 1973, Bažant 1971). The development of sophisticated micromechanical material models has also stimulated an increased interest in the mechanical properties of random structures. One approach to this problem utilizes the theory of micropolar elasticity (Eringen 1966) within the framework of latice percolation theory (Feng 1985, Limat 1988a). Within the framework of this theory a characteristic length is associated with the material, and the stress and strain tensors are generally non-symmetric. In two-dimensional material models these microstructures are often represented by hexagonal and equilateral triangle geometries which exhibit three-fold symmetry in the plane. It is well known that for simple materials this three-fold symmetry insures mechanical isotropy in the plane (Christensen 1987).

In this work we investigate the form of the two-dimensional linear constitutive relations which this symmetry condition imposes on micropolar materials. Following a summary of the two-dimensional field equations for micropolar materials, we consider the effects of rotations of the reference configuration in the plane on the general form of these linear constitutive relations. We show that the three-fold symmetry condition requires that the stresses be isotropic in the plane. These non-symmetric isotropic stresses are defined by 6 elastic constants relating the components of strain to stress, and no strain gradient effects are possible. If the material is assumed hyperelastic, these 6 constants are reduced to 4. For non-micropolar materials, the stress and strain tensors are symmetric and the number of constants reduces to 2 which is characteristic of the well known linear elastic isotropic material. The two-dimensional couple stresses are also isotropic in the plane and are related to the strain and rotation gradients by 8 independent constants. These couple stresses depend only on the strain and rotation gradients and are independent of the strain components.

After establishing the form of the constitutive relations for two-dimensional micropolar materials which exhibit three-fold symmetry, we obtain specific constitutive relations for an equilateral triangle structure and for a hexagonal or honeycomb structure. These results are compared with the results of previous

investigations of these two-dimensional material models.

2 General Two-Dimensional Theory

Within the kinematically linear theory of micropolar media (Eringen 1966), (Christoffersen 1996), the strain-displacement relations with respect to a two-dimensional Cartesian reference frame (x, y) are given by

$$\varepsilon_{xx} = \frac{\partial u}{\partial x} \; , \quad \varepsilon_{xy} = \frac{\partial v}{\partial x} - \psi \; , \quad \varepsilon_{yx} = \frac{\partial u}{\partial y} + \psi \; , \quad \varepsilon_{yy} = \frac{\partial v}{\partial y} \tag{1}$$

$$\kappa_{xz} = \frac{\partial \psi}{\partial x} \; , \quad \kappa_{yz} = \frac{\partial \psi}{\partial y}$$

where u, v are the displacements in the x- and y-directions, respectively, ψ is the rotation about the normal to the x-y-plane, $\varepsilon_{\alpha\beta}$, $(\alpha, \beta) = (x, y)$ denotes the direct strain tensor, and $\kappa_{\alpha\beta}$ is the curvature strain tensor. Compatibility is satisfied if

$$\frac{\partial \varepsilon_{yx}}{\partial x} - \frac{\partial \varepsilon_{xx}}{\partial y} - \kappa_{xz} = 0 \; , \quad \frac{\partial \varepsilon_{yy}}{\partial x} - \frac{\partial \varepsilon_{xy}}{\partial y} - \kappa_{yz} = 0 \tag{2}$$

$$\frac{\partial \kappa_{yz}}{\partial x} - \frac{\partial \kappa_{xz}}{\partial y} = 0$$

Equilibrium requires

$$\frac{\partial \sigma_{xx}}{\partial x} + \frac{\partial \sigma_{yx}}{\partial y} + p_x = 0 \; , \quad \frac{\partial \sigma_{xy}}{\partial x} + \frac{\partial \sigma_{yy}}{\partial y} + p_y = 0 \tag{3}$$

$$\frac{\partial \mu_{xz}}{\partial x} + \frac{\partial \mu_{yz}}{\partial y} + \sigma_{xy} - \sigma_{yx} + q_z = 0$$

where $\sigma_{\alpha\beta}$ denotes the direct stress tensor, $\mu_{\alpha\beta}$ the couple stress, p_α the body force, and q_α the body couple. In general, $\sigma_{\alpha\beta}$ and $\mu_{\alpha\beta}$ are not symmetric.

3 Three-Fold Symmetry Condition

We consider here the form of the linear micropolar constitutive relations which the three-fold symmetry condition imposes. With respect to a Cartesian reference frame (x,y) in the plane, the components of the micropolar strain tensor are given by (1). To simplify the strain transformations, we introduce the strain combinations

$$L_1 = \varepsilon_{xx} + \varepsilon_{yy} \; , \quad L_2 = \varepsilon_{xx} - \varepsilon_{yy} \; , \tag{4}$$

$$L_3 = \varepsilon_{xy} + \varepsilon_{yx} \; , \quad L_4 = \varepsilon_{xy} - \varepsilon_{yx}$$
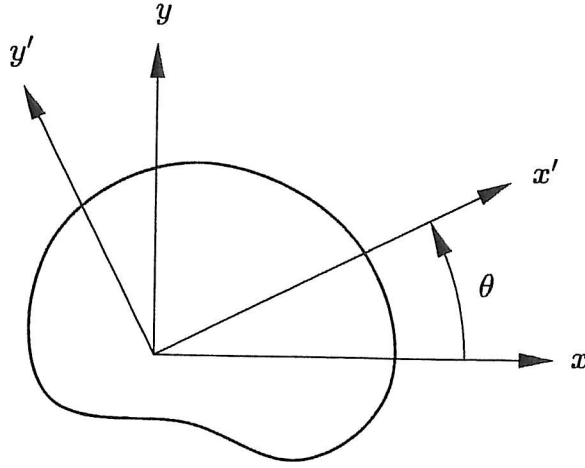
Fig. 1. Change of two-dimensional reference frame from (x, y) to (x', y') through a counterclockwise rotation θ.

and consider a rotation of the reference frame from (x, y) to (x', y') counterclockwise through the angle θ as shown in Fig. 1. The strain combinations of (4) transform as

$$L_1 = L_1' \,, \qquad L_2 = \cos(2\theta)L_2' - \sin(2\theta)L_3' \,,$$
$$L_3 = \sin(2\theta)L_2' + \cos(2\theta)L_3' \,, \qquad L_4 = L_4' \tag{5}$$

and the stresses $\sigma_{xx}, \sigma_{xy}, \sigma_{yx}, \sigma_{yy}$ transform as

$$\sigma_{x'x'} + \sigma_{y'y'} = \sigma_{xx} + \sigma_{yy} \,, \qquad \sigma_{x'y'} - \sigma_{y'x'} = \sigma_{xy} - \sigma_{yx} \,, \tag{6}$$
$$\sigma_{y'y'} - \sigma_{x'x'} = (\sigma_{yy} - \sigma_{xx})\cos(2\theta) - (\sigma_{xy} - \sigma_{yx})\sin(2\theta) \,,$$
$$\sigma_{x'y'} + \sigma_{y'x'} = (\sigma_{xy} + \sigma_{yx})\cos(2\theta) + (\sigma_{yy} - \sigma_{xx})\sin(2\theta)$$

We assume a general linear stress-strain relation in the (x, y) frame to be of the form

$$\sigma_{\alpha\beta} = \alpha_{\alpha\beta m}L_m + \beta_{\alpha\beta\gamma m}L_{m,\gamma} + \gamma_{\alpha\beta\gamma}\psi_{,\gamma} \tag{7}$$

where Greek indices $\alpha, \beta, \gamma = 1, 2$ and the Latin index $m = 1, \ldots, 4$. Threefold symmetry requires that the form of this constitutive relation be the same for rotations of $\theta = \pm 60°$ and $\theta = 180°$. The reflective condition at $\theta = 180°$ requires all $\beta_{\alpha\beta\gamma m} = 0$ and $\gamma_{\alpha\beta\gamma} = 0$, while the three-fold symmetry condition

demands

$$
\begin{aligned}
\alpha_{111} &= \alpha_{221} = a_1 \\
\alpha_{112} &= -\alpha_{222} = \alpha_{123} = \alpha_{213} = a_2 \\
\alpha_{113} &= -\alpha_{223} = -\alpha_{122} = -\alpha_{212} = a_3 \\
\alpha_{114} &= \alpha_{224} = a_4 \\
\alpha_{121} &= -\alpha_{221} = a_5 \\
\alpha_{124} &= -\alpha_{214} = a_6
\end{aligned}
\tag{8}
$$

The stresses are given by

$$
\begin{aligned}
\sigma_{xx} &= a_1 L_1 + a_2 L_2 + a_3 L_3 + a_4 L_4 \\
\sigma_{xy} &= a_5 L_1 - a_3 L_2 + a_2 L_3 + a_6 L_4 \\
\sigma_{yx} &= -a_5 L_1 - a_3 L_2 + a_2 L_3 - a_6 L_4 \\
\sigma_{yy} &= a_1 L_1 - a_2 L_2 - a_3 L_3 + a_4 L_4
\end{aligned}
\tag{9}
$$

where the a_i are the 6 independent material constants. The stresses of (9) are isotropic in the plane. If the material is assumed to be hyperelastic, $a_3 = 0, a_5 = a_4$, and the number of elastic constants reduces to 4. We note that if the stress and strain tensors are symmetric, representing a simple linear elastic material, (9) has the usual 2 independent constants.

For a rotation of the reference frame counnterclockwise through the angle θ as shown in Fig. 1, the couple stresses μ_{xz} and μ_{yz} transform as

$$
\mu_{x'z} = \mu_{xz} \cos\theta + \mu_{yz} \sin\theta , \quad \mu_{y'z} = -\mu_{xz} \sin\theta + \mu_{yz} \cos\theta
\tag{10}
$$

We assume a general linear couple-stress relation in the (x, y) frame to be of the form

$$
\mu_{\alpha 3} = A_{\alpha\beta} \psi_{,\beta} + B_{\alpha\beta m} L_{m,\beta} + \Gamma_{\alpha m} L_m
\tag{11}
$$

with greek indices taking the values $(1, 2)$ and the Latin index m the values $1, \ldots, 4$, as before. Three-fold symmetry again requires that the form of this constitutive relation be the same for rotations of $\theta = \pm 60°$ and $\theta = 180°$. The reflective condition at $\theta = 180°$ requires all $\Gamma_{\alpha m} = 0$, and the three-fold symmetry condition demands

$$
\begin{aligned}
A_{11} &= A_{22} = b_1 , & A_{12} &= -A_{21} = b_2 \\
B_{111} &= B_{221} = b_3 , & B_{121} &= -B_{211} = b_4 \\
B_{112} &= B_{123} = -B_{222} = B_{213} = b_5 \\
B_{122} &= -B_{113} = B_{212} = B_{223} = b_6 \\
B_{114} &= B_{224} = b_7 , & B_{124} &= -B_{214} = b_8
\end{aligned}
\tag{12}
$$

The couple stresses are given by

$$\mu_{xz} = + b_1\psi_{,x} + b_2\psi_{,y} + b_3 L_{1,x} + b_4 L_{1,y} + b_5(L_{2,x} + L_{3,y}) \tag{13}$$
$$+ b_6(L_{2,y} - L_{3,x}) + b_7 L_{4,x} + b_8 L_{4,y}$$

$$\mu_{yz} = - b_2\psi_{,x} + b_1\psi_{,y} - b_4 L_{1,x} + b_3 L_{1,y} - b_5(L_{2,y} - L_{3,x})$$
$$+ b_6(L_{2,x} + L_{3,y}) - b_8 L_{4,x} + b_7 L_{4,y}$$

where the 8 b_i are material constants. The couple stresses of (13) are isotropic in the plane. We note here that previous investigations of the micropolar behavior of honeycombs have generally retained only the b_1 term, see e.g. (Chen, Huang & Ortiz 1998) and (Wang & Stronge 1999). Our results for specific structures indicate that this is a realistic assumption.

We now develop the specific micropolar continuum field equations representative of the mechanical response of two separate discrete two-dimensional lattice geometries, both of which exhibit three-fold symmetry in the plane. These structures are assumed spatially periodic and connected, and force and moment equilibrium are explicitly enforced at each joint. Since we are interested only in deformations occurring under static loading conditions, the actual mass distribution within the structure is unimportant and will be assumed uniformly distributed and concentrated at each joint. These mass points (joints) are connected by thin beams which deform by stretching and bending. Thus we are starting with a structure in which each discrete material point is defined within the structure by both its position and its orientation, the position and orientation being independent of each other. For example, in our two-dimensional structure defined in the Cartesian coordinate system (x, y), deformation of the mass point m_i is defined by the independent triad (u_i, v_i, ψ_i), where u_i is the displacement in the x-direction, v_i the displacement in the y-direction, and ψ_i is the rotation in the out-of plane direction. Our goal is to represent the mechanical behavior of this discrete structure in terms of a continuum, and this transition from discrete to continuous depends on a characteristic length, here taken as the length a of the beam connecting the mass point. As this length parameter approaches zero, microstructural effects are expected to vanish and the material is characterized as a simple material in which the orientation of a material point is not independent of the deformation of its neighbors. In the absence of microstructure, each material point in the continuum is defined by u, v, and the rotation ψ is equal to the local infinitesimal rigid body rotation $\omega = \frac{1}{2}(v_{,x} - u_{,y})$. For the two lattice geometries investigated here, we show that as $a \to 0$, this condition on the rotation is satisfied. We also assume that if c is a length scale associated with the deformation pattern of the structure under investigation, the following condition is valid $(a/c) \ll 1$.

To effect this transition from discrete structure to continuum we utilize the procedure developed by Mindlin (1968) and make use of Taylor series ex-

pansions of the displacements and rotations about a material point within the structure. This presumes that the functional representation of these terms is differentiable with respect to the space variables as often as necessary. We show that it is necessary to retain second order terms in the series expansions in order to induce micropolar effects in the two lattice geometries investigated here. Suppressing second order terms in the displacement expansions is equivalent to assuming homogeneous displacements and a uniform strain field, and micropolar material effects do not appear to be possible in a uniform strain field.

4 Equilateral Triangle Structure

4.1 Description of the Equilateral Triangle Structure

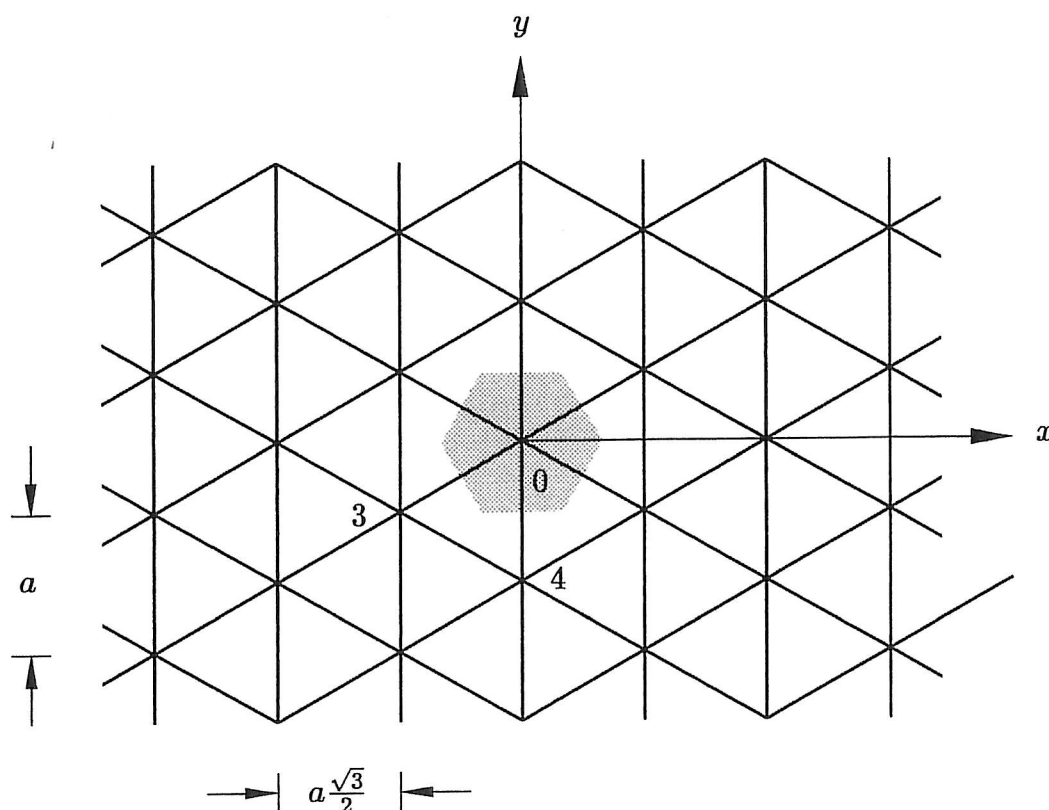**Fig. 2.** Geometry of the spatially periodic equilateral triangle lattice with the representative volume element as shown.

We consider the spatially periodic structure made up of equilateral triangles as shown in Fig. 2. A representative volume element of this structure is also shown, and we take the fundamental element of this structure to be the equilateral triangle element shown in Fig. 3. Deformations of this structure
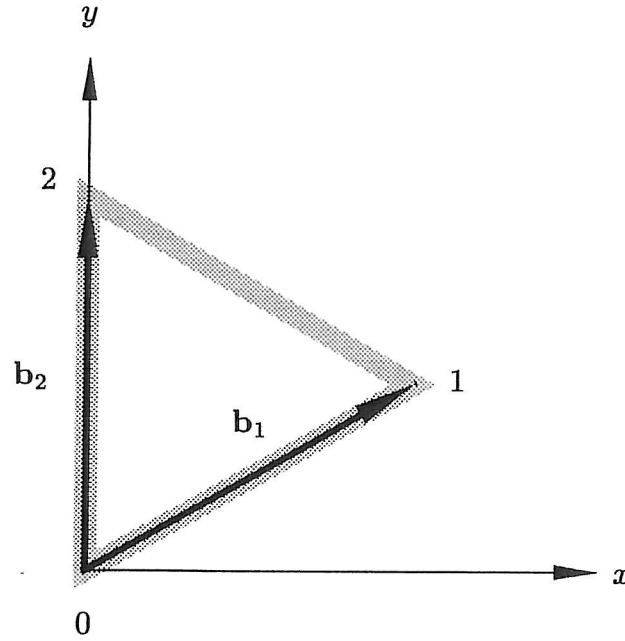
Fig. 3. Fundamental structural element.

are defined by the relative motion of points 1 and 2 with respect to the point 0 through the position vectors $\mathbf{b}_1$ and $\mathbf{b}_2$. We restrict our investigation to small deformations from the initial shape. The motion of points 0, 1, 2 are represented by a displacement u in the x direction, a displacement v in the y direction, and a rotation ψ in the z direction. Thus the motion of point 0 is defined by the triad (u_0, v_0, ψ_0), the motion of point 1 by (u_1, v_1, ψ_1), and the motion of point 2 by (u_2, v_2, ψ_2). A representative beam, the beam connecting joints 0 and 1, is shown in Fig. 4 along with the forces and moments acting at the ends. These consist of an axial force P, a transverse force T, and a beam midpoint moment M with positive directions as shown. The beam connecting joints 0 and 1 will be denoted as beam 1, that connecting joints 0 and 2 as beam 2, and that connecting joints 1 and 2 as beam 3.

We assume all beams to have length a and uniform thickness t such that the ratio $t/a \ll 1$. Thus this structure can be considered to be a form of two-dimensional low density foam with volume fraction $\phi = 2\sqrt{3}(t/a)$. The beams are assumed to undergo linear elastic deformations of simple stretching due to the axial forces P, and Bernoulli-Euler bending due to the moments M and transverse forces T. In terms of the joint displacements and rotations, the
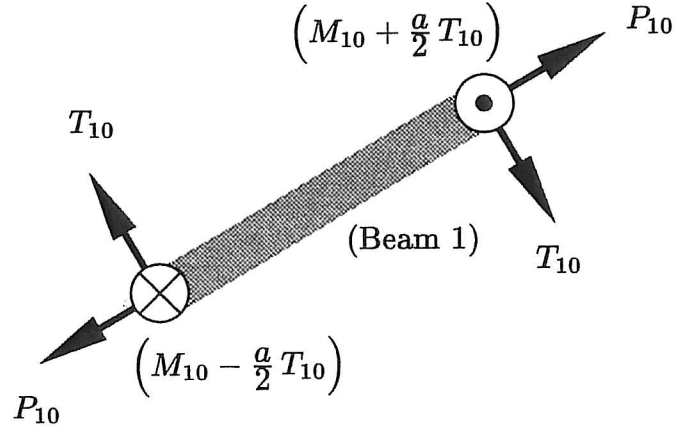
Fig. 4. Forces and moments on one of the beams of the structural element with sign conventions as indicated.

forces and moments in beam 1 are

$$P_{10} = \frac{EA}{2a}\left(\sqrt{3}(u_1 - u_0) + (v_1 - v_0)\right)$$

$$T_{10} = \frac{6EI}{a^3}\left((u_1 - u_0) - \sqrt{3}(v_1 - v_0) + a(\psi_1 + \psi_0)\right) \tag{14}$$

$$M_{10} = \frac{EI}{a}(\psi_1 - \psi_0)$$

Similarly, the forces and moments in beam 2 are

$$P_{20} = \frac{EA}{a}(v_2 - v_0)$$

$$T_{20} = \frac{6EI}{a^3}(2(u_2 - u_0) + a(\psi_2 + \psi_0)) \tag{15}$$

$$M_{20} = \frac{EI}{a}(\psi_2 - \psi_0),$$

and in beam 3,

$$P_{21} = \frac{EA}{2a}\left(-\sqrt{3}(u_2 - u_1) + (v_2 - v_1)\right)$$

$$T_{21} = \frac{6EI}{a^3}\left((u_2 - u_1) + \sqrt{3}(v_2 - v_1) + a(\psi_2 + \psi_1)\right) \tag{16}$$

$$M_{21} = \frac{EI}{a}(\psi_2 - \psi_1).$$

This solution of the statically indeterminate structure problem satisfies compatibility of displacements and rotations at the joints.

To effect a continuum representation of this structure, we now assume the existence of continuous displacement fields $u(x, y)$ and $v(x, y)$, and a continuous rotation field $\psi(x, y)$ such that the displacements and rotations of joints 1 and 2 can be expressed as Taylor series about the joint 0. This presumes that the displacement and rotation fields are differentiable to whatever order necessary, and

$$
\begin{aligned}
(u_1 - u_0) &= \frac{a\sqrt{3}}{2}\frac{\partial u}{\partial x} + \frac{a}{2}\frac{\partial u}{\partial y} + \frac{a^2}{8}\left(3\frac{\partial^2 u}{\partial x^2} + 2\sqrt{3}\frac{\partial^2 u}{\partial x \partial y} + \frac{\partial^2 u}{\partial y^2}\right) + \cdots \\[2mm]
(v_1 - v_0) &= \frac{a\sqrt{3}}{2}\frac{\partial v}{\partial x} + \frac{a}{2}\frac{\partial v}{\partial y} + \frac{a^2}{8}\left(3\frac{\partial^2 v}{\partial x^2} + 2\sqrt{3}\frac{\partial^2 v}{\partial x \partial y} + \frac{\partial^2 v}{\partial y^2}\right) + \cdots \\[2mm]
(\psi_1 - \psi_0) &= \frac{a\sqrt{3}}{2}\frac{\partial \psi}{\partial x} + \frac{a}{2}\frac{\partial \psi}{\partial y} + \frac{a^2}{8}\left(3\frac{\partial^2 \psi}{\partial x^2} + 2\sqrt{3}\frac{\partial^2 \psi}{\partial x \partial y} + \frac{\partial^2 \psi}{\partial y^2}\right) + \cdots \\[2mm]
(u_2 - u_0) &= a\frac{\partial u}{\partial y} + \frac{a^2}{2}\frac{\partial^2 u}{\partial y^2} + \cdots \\[2mm]
(v_2 - v_0) &= a\frac{\partial v}{\partial y} + \frac{a^2}{2}\frac{\partial^2 v}{\partial y^2} + \cdots \\[2mm]
(\psi_2 - \psi_0) &= a\frac{\partial \psi}{\partial y} + \frac{a^2}{2}\frac{\partial^2 \psi}{\partial y^2} + \cdots,
\end{aligned}
$$

$$(17)$$

where we have retained terms of order a^2, and all derivatives are evaluated at the point 0. We note that

$$(u_2 - u_1) = (u_2 - u_0) - (u_1 - u_0) \tag{18}$$

with similar expression involving v_i and ψ_i.

With the displacements and rotations expressed by (17), the forces and

moments in beam 1 become

$$P_{10} = \frac{EA}{4} \left\{ 3\frac{\partial u}{\partial x} + \frac{\partial v}{\partial y} + \sqrt{3}\left(\frac{\partial u}{\partial y} + \frac{\partial v}{\partial x}\right) \right.$$
$$+ \frac{a\sqrt{3}}{4}\left(3\frac{\partial^2 u}{\partial x^2} + 2\sqrt{3}\frac{\partial^2 u}{\partial x \partial y} + \frac{\partial^2 u}{\partial y^2}\right)$$
$$\left. + \frac{a}{4}\left(3\frac{\partial^2 v}{\partial x^2} + 2\sqrt{3}\frac{\partial^2 v}{\partial x \partial y} + \frac{\partial^2 v}{\partial y^2}\right) \right\}$$

$$T_{10} = \frac{3EI}{a^2} \left\{ \sqrt{3}\left(\frac{\partial u}{\partial x} - \frac{\partial v}{\partial y}\right) - \left(\frac{\partial u}{\partial y} + \frac{\partial v}{\partial x}\right) + 2\left(2\psi + \frac{\partial u}{\partial y} - \frac{\partial v}{\partial x}\right) \right.$$
$$+ a\sqrt{3}\frac{\partial \psi}{\partial x} + a\frac{\partial \psi}{\partial y} + \frac{a}{4}\left(3\frac{\partial^2 u}{\partial x^2} + 2\sqrt{3}\frac{\partial^2 u}{\partial x \partial y} + \frac{\partial^2 u}{\partial y^2}\right)$$
$$\left. - \frac{a\sqrt{3}}{4}\left(3\frac{\partial^2 v}{\partial x^2} + 2\sqrt{3}\frac{\partial^2 v}{\partial x \partial y} + \frac{\partial^2 v}{\partial y^2}\right) \right\}$$

$$M_{10} = \frac{EI}{2} \left\{ \sqrt{3}\frac{\partial \psi}{\partial x} + \frac{\partial \psi}{\partial y} + \frac{a}{4}\left(3\frac{\partial^2 \psi}{\partial x^2} + 2\sqrt{3}\frac{\partial^2 \psi}{\partial x \partial y} + \frac{\partial^2 \psi}{\partial y^2}\right) \right\},$$

$$(19)$$

and similarly in beam 2

$$P_{20} = EA\left\{ \frac{\partial v}{\partial y} + \frac{a}{2}\frac{\partial^2 v}{\partial y^2} \right\}$$

$$T_{20} = \frac{6EI}{a^2} \left\{ \left(\frac{\partial u}{\partial y} + \frac{\partial v}{\partial x}\right) + \left(2\psi + \frac{\partial u}{\partial y} - \frac{\partial v}{\partial x}\right) \right.$$
$$\left. + a\frac{\partial \psi}{\partial y} + a\frac{\partial^2 u}{\partial y^2} \right\}$$

$$(20)$$

$$M_{20} = EI\left(\frac{\partial \psi}{\partial y} + \frac{a}{2}\frac{\partial^2 \psi}{\partial y^2}\right),$$

and finally in beam 3

$$
P_{21} = \frac{EA}{4} \left\{ 3\frac{\partial u}{\partial x} + \frac{\partial v}{\partial y} - \sqrt{3}\left(\frac{\partial u}{\partial y} + \frac{\partial v}{\partial x}\right) \right.
$$

$$
+ \frac{a\sqrt{3}}{4}\left(3\frac{\partial^2 u}{\partial x^2} + 2\sqrt{3}\frac{\partial^2 u}{\partial x \partial y} - 3\frac{\partial^2 u}{\partial y^2}\right)
$$

$$
\left. - \frac{a}{4}\left(3\frac{\partial^2 v}{\partial x^2} + 2\sqrt{3}\frac{\partial^2 v}{\partial x \partial y} - 3\frac{\partial^2 v}{\partial y^2}\right) \right\}
$$

$$
T_{21} = \frac{3EI}{a^2} \left\{ -\sqrt{3}\left(\frac{\partial u}{\partial x} - \frac{\partial v}{\partial y}\right) - \left(\frac{\partial u}{\partial y} + \frac{\partial v}{\partial x}\right) \right.
$$

$$
+ 2\left(2\psi + \frac{\partial u}{\partial y} - \frac{\partial v}{\partial x}\right) + a\sqrt{3}\frac{\partial \psi}{\partial x} + 3a\frac{\partial \psi}{\partial y}
$$

$$
- \frac{a}{4}\left(3\frac{\partial^2 u}{\partial x^2} + 2\sqrt{3}\frac{\partial^2 u}{\partial x \partial y} - 3\frac{\partial^2 u}{\partial y^2}\right)
$$

$$
\left. - \frac{a\sqrt{3}}{4}\left(3\frac{\partial^2 v}{\partial x^2} + 2\sqrt{3}\frac{\partial^2 v}{\partial x \partial y} - 3\frac{\partial^2 v}{\partial y^2}\right) \right\}
$$

$$
M_{21} = -\frac{EI}{2}\left\{ \sqrt{3}\frac{\partial \psi}{\partial x} - \frac{\partial \psi}{\partial y} + \frac{a}{4}\left(3\frac{\partial^2 \psi}{\partial x^2} + 2\sqrt{3}\frac{\partial^2 \psi}{\partial x \partial y} - 3\frac{\partial^2 \psi}{\partial y^2}\right) \right\}.
$$

(21)

The representative volume element of Fig. 2 is shown in more detail in Fig. 5. The boundary of this element passes through midpoints as shown. The forces and moments in the 3 beams associated with the joint 0 are given by (19), (20), (21). The forces and moments in the remaining beams within the representative element are obtained from Taylor series expansions about the joint 0 of these three known forces. These expansions are consistent with our assumption that the displacement and rotation fields are differentiable as often as necessary. For example, the forces and moments in the beams associated with the joint 3 of Fig. 2, located at the point $(-\sqrt{3}a/2, -a/2)$ with respect to the joint 0, are denoted by P_{13}, T_{13}, M_{13} etc. and are given by

$$
P_{13} = P_{10} - \frac{a\sqrt{3}}{2}\frac{\partial P_{10}}{\partial x} - \frac{a}{2}\frac{\partial P_{10}}{\partial y} + \cdots
$$

$$
T_{13} = T_{10} - \frac{a\sqrt{3}}{2}\frac{\partial T_{10}}{\partial x} - \frac{a}{2}\frac{\partial T_{10}}{\partial y} + \cdots
$$

(22)

$$
M_{13} = M_{10} - \frac{a\sqrt{3}}{2}\frac{\partial M_{10}}{\partial x} - \frac{a}{2}\frac{\partial M_{10}}{\partial y} + \cdots
$$
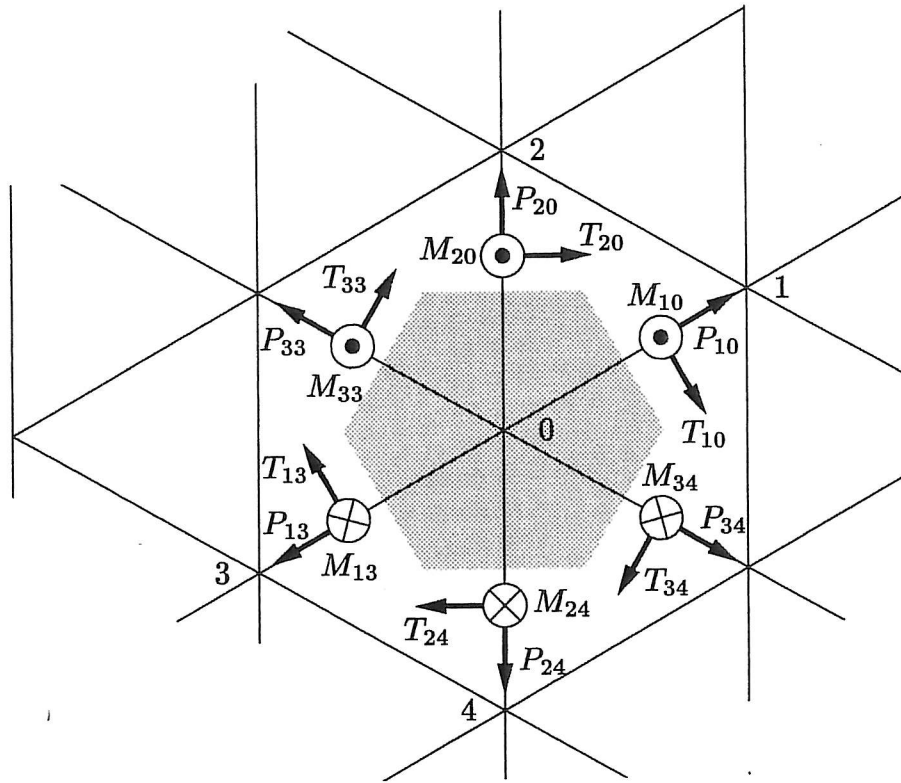
Fig. 5. Representative volume element for the equilateral triangle structure with resultant forces and moments on the six faces.

with similar expressions for the forces and moments in the other beams. All variables are evaluated at the center of the element. This procedure determines all forces and moments in the beams of the representative volume element.

4.2   Effective Stresses

The effective stresses and couple stresses are determined by volume averaging the forces and moments acting on the boundary of the representative volume element. The volume averaged stresses $\bar{\sigma}_{\alpha\beta}$ are given by

$$V\bar{\sigma}_{\alpha\beta} = \sum_{n=1}^{N} x_\alpha^n F_\beta^n \tag{23}$$

where $V = a^2\sqrt{3}/2$ is the area of the representative volume element.

Using (23), the stresses become

$$\bar{\sigma}_{xx} = \frac{\sqrt{3}}{8}\left\{\frac{2}{M}L_1 + \frac{(M+N)}{MN}L_2\right\}$$

$$\bar{\sigma}_{yy} = \frac{\sqrt{3}}{8}\left\{\frac{2}{M}L_1 - \frac{(M+N)}{MN}L_2\right\}$$

$$(\bar{\sigma}_{xy} + \bar{\sigma}_{yx}) = \frac{\sqrt{3}}{4}\frac{(M+N)}{MN}L_3 \tag{24}$$

$$(\bar{\sigma}_{xy} - \bar{\sigma}_{yx}) = \frac{\sqrt{3}}{2N}L_4$$

To evaluate these stresses and couple stresses, we have introduced the beam stretching compliance M and the beam bending compliance N such that

$$2M = \frac{a}{EA} = \frac{1}{E}\left(\frac{a}{t}\right), \quad 2N = \frac{a^3}{12EI} = \frac{1}{E}\left(\frac{a}{t}\right)^3, \tag{25}$$

where, per unit depth, $A = t$ and $I = t^3/12$. We note that for low density materials with $t/a \ll 1$, the bending compliance N is much greater than the stretching compliance M, i.e. $N \gg M$.

An alternative estimate of the shear stress difference $(\bar{\sigma}_{xy} - \bar{\sigma}_{yx})$ can also be obtained from the moment equilibrium equation (3c). We have

$$\mu_{ik,i} + e_{kij}\sigma_{ij} = 0 \tag{26}$$

and integrating this over the representative volume element and utilizing the divergence theorem provides

$$\int_V \mu_{ik,i}dV + e_{kij}\int_V \sigma_{ij}dV = 0$$

or

$$\int_S \mu_{ik}n_i dS + e_{kij}V\sigma_{ij} = 0$$

and

$$\int_S m_k dS + e_{kij}V\sigma_{ij} = 0 .$$

For concentrated moments M_k^n at N points on the boundary, we get

$$\sum_{n=1}^{N}M_k^n + e_{kij}V\bar{\sigma}_{ij} = 0 \tag{27}$$

For our two-dimensional system with $k = 3$ (z), (27) gives

$$V(\bar{\sigma}_{xy} - \bar{\sigma}_{yx}) = -\sum_{n=1}^{N} M_z^n \tag{28}$$

Evaluation of (28) provides

$$\bar{\sigma}_{xy} - \bar{\sigma}_{yx} = -\frac{a^2\sqrt{3}}{24N}\nabla^2\psi \tag{29}$$

and the two expressions for the shear stress difference as given by (29) and (24) provides the moment equilibrium relation

$$L_4 = -\frac{a^2}{12}\nabla^2\psi$$

or

$$\left(2\psi + \frac{\partial u}{\partial y} - \frac{\partial v}{\partial x}\right) - \frac{a^2}{12}\nabla^2\psi = 0 \tag{30}$$

We note that the shear stress difference is of order a^2 compared with the other stresses of (24).

Volume averaged expressions for the couple stresses can be obtained from the moment equilibrium equation. We multiply (26) by x_l to get

$$\mu_{ik,i}x_l + e_{kij}\sigma_{ij}x_l = 0 \tag{31}$$

We now integrate this expression over the representative volume element

$$\int_V \mu_{ik,i}x_l dV + e_{kij}\int_V \sigma_{ij}x_l dV = 0$$

$$\int_V \left[(\mu_{ik}x_l)_{,i} - \mu_{ik}x_{l,i}\right] dV + e_{kij}\int_V \sigma_{ij}x_l dV = 0$$

and apply the divergence theorem to the first term to get

$$\int_S \mu_{ik,i}x_l n_i dS - \int_V \mu_{lk} dV + e_{kij}\int_V \sigma_{ij}x_l dV = 0 \tag{32}$$

and finally

$$V\bar{\mu}_{lk} = \int_S m_k x_l dS + e_{kij}\int_V \sigma_{ij}x_l dV = 0 \tag{33}$$

For a system of concentrated moments acting on the surface S of the volume V, the integration over the surface reduces to a summation over the concentrated moments. For our two-dimensional geometry we take $k = 3$ and $l = 1, 2$ in (33) to get the representations

$$\bar{\mu}_{13} = \sum_{n=1}^{N} x_1^n M_3^n dS + \int_V (\sigma_{12} - \sigma_{21}) x_1 dV$$

$$\bar{\mu}_{23} = \sum_{n=1}^{N} x_2^n M_3^n dS + \int_V (\sigma_{12} - \sigma_{21}) x_2 dV \tag{34}$$

The integrals of (34) are not readily evaluated. However, these integrals are of order a^5 which is higher than the moment terms which are of order a^4. Suppressing the integrals of (34) gives the couple stresses

$$\bar{\mu}_{xz} = \frac{a^2}{8\sqrt{3}N} \frac{\partial \psi}{\partial x}$$

$$\bar{\mu}_{yz} = \frac{a^2}{8\sqrt{3}N} \frac{\partial \psi}{\partial y} \tag{35}$$

The relations of (24) and (35) provide the constitutive equations for the equilateral triangle structure which satisfy the three-fold symmetry conditions. For this structure, the coefficients of (9) and (13) are

$$a_1 = \frac{\sqrt{3}}{4M} \ , \quad a_2 = \frac{\sqrt{3}(M+N)}{8MN} \ , \quad a_3 = a_4 = a_5 = 0 \ , \quad a_6 = \frac{\sqrt{3}}{4N} \tag{36}$$

and

$$b_1 = \frac{a^2\sqrt{3}}{24N} \ , \quad b_2 = b_3 = b_4 = b_5 = b_6 = b_7 = b_8 = 0 \tag{37}$$

respectively.

We note that as the strut length $a \to 0$, $\bar{\mu}_{xz} \to 0$, $\bar{\mu}_{yz} \to 0$ and $L_4 \to 0$. The constitutive relations (24) are then representative of a simple material which is isotropic in the plane.

4.3   Example—Simple Bending

As an example of the stresses developed during deformation of this structure, we consider the response to a simple bending deformation defined by Fig. 6

$$u = -kyx \ , \quad v = \frac{1}{2}k\left[x^2 + \frac{(N-M)}{(3N+M)}y^2\right] \ , \quad \psi = kx \tag{38}$$
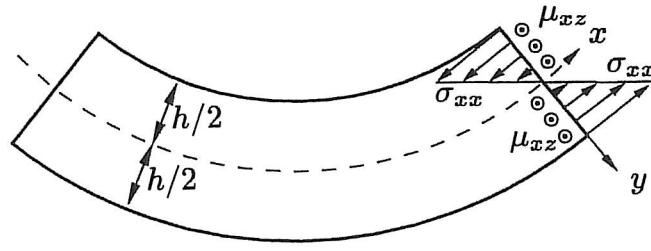
Fig. 6. Simple bending of a strip.

where k is the curvature of the bent material. For this equilateral triangle structure under conditions of simple bending there is a definite micropolar effect since

$$L_1 = -\frac{2(N+M)}{(3N+M)}ky \,, \quad L_2 = -\frac{4N}{(3N+M)}ky \,, \quad L_3 = 0 \,, \quad L_4 = 0 \quad (39)$$

$$\bar{\sigma}_{xx} = -\frac{\sqrt{3}(N+M)}{M(3N+M)}ky \,, \quad \bar{\sigma}_{xy} = \bar{\sigma}_{yx} = \bar{\sigma}_{yy} = 0 \,, \quad (40)$$

and

$$\bar{\mu}_{xz} = \frac{a^2}{8\sqrt{3}N}k \,, \quad \bar{\mu}_{yz} = 0 \quad (41)$$

We note that as the strut length $a \to 0$ the micropolar effect vanishes and the rotation ψ becomes equal to the local infinitesimal rigid rotation.

We observe that couple stresses are induced on surfaces with normal in the x-direction. Thus this stress and displacement field is representative of the response of a rectangular beam of depth h, width b, and length l bent with uniform curvature k, see Fig. 6. The moment $\mathcal{M}$ which must be applied at the ends of the beam to support this deformation is given by

$$\mathcal{M} = \frac{(N+M)kbh^3}{4\sqrt{3}M(3N+M)}\left[1 + \frac{M(3N+M)}{2(N+M)^2}\left(\frac{a}{h}\right)^2\right] \quad (42)$$

The second term in the brackets represent the global effect of the couple stress μ_{xz} on the simple bending of a beam made of material with equilateral triangle structure. Note that in deriving the above expressions we assume that the characteristic length a is small compared to the overall dimensions of the structure under investigation which for this problem implies that $(a/h) \ll 1$. For typical structures of this type, $(t/a) \ll 1$ and the bending compliance N is much greater than the stretching compliance M, i.e. $N \gg M$. Under these conditions, the moment $\mathcal{M}$ becomes

$$\mathcal{M} = \frac{kbh^3}{12\sqrt{3}M}\left[1 + \frac{3M}{2N}\left(\frac{a}{h}\right)^2\right] \quad (43)$$

5   Hexagonal Structure
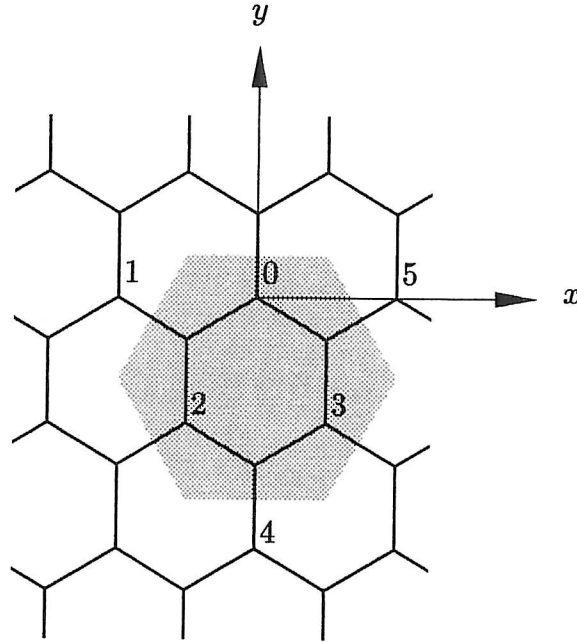
5.1   Forces and Moments in Beams

Fig. 7. Spatially periodic hexagonal lattice with the representative volume element shown shaded.

We consider the spatially periodic hexagonal structure as shown in Fig. 7, in which a representative volume element of this structure is also shown. The fundamental element of this structure is shown in Fig. 8 and consists of three beams emanating from the joint 0 at equal angles of 120° from each other. Note that the fundamental element is only a subset of the representative volume element. Deformations of the fundamental element are defined by the relative motion of points 1 and 2 with respect to the point 3 through the position vectors b_1 and b_2 as shown. The motion of point 1 is defined by the triad (u_1, v_1, ψ_1) with similar representations for the motion of points 0, 2 and 3. The individual beams connecting the joints have forces and moments acting at the ends similar to those shown in Fig. 4 for the equilateral triangle. The beam connecting the joints 0 and 1 will be denoted as beam 10, that connecting joints 0 and 2 as beam 20, and that connecting joints 0 and 3 as beam 30.

The forces and moments in these beams are expressed in terms of the
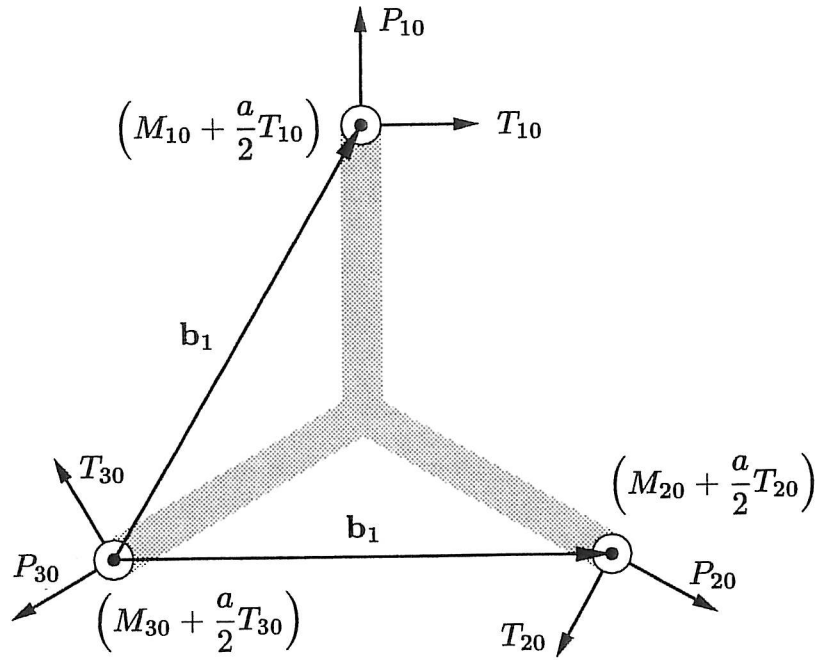
Fig. 8. Fundamental structural element for the hexagonal lattice with position vectors $\mathbf{b}_1$ and $\mathbf{b}_2$. Force and moment conventions as shown.

displacements and rotations of the ends (joints) and take the form

$$P_{10} = \frac{EA}{a}(v_1 - v_0)$$

$$T_{10} = \frac{6EI}{a^3}\left(2(u_1 - u_0) + a(\psi_1 + \psi_0)\right) \tag{44}$$

$$M_{10} = \frac{EI}{a}(\psi_1 - \psi_0),$$

where the double subscript 10 indicates effects in beam 1 as referred to the joint 0. Similarly, the forces and moments in beam 2 are

$$P_{20} = \frac{EA}{2a}\left(\sqrt{3}(u_2 - u_0) - (v_2 - v_0)\right)$$

$$T_{20} = -\frac{6EI}{a^3}\left((u_2 - u_0) + \sqrt{3}(v_2 - v_0) - a(\psi_2 + \psi_0)\right) \tag{45}$$

$$M_{20} = \frac{EI}{a}(\psi_2 - \psi_0).$$

and in beam 3,

$$P_{30} = -\frac{EA}{2a}\left(\sqrt{3}(u_3 - u_0) + (v_3 - v_0)\right)$$

$$T_{30} = \frac{6EI}{a^3}\left(-(u_3 - u_0) + \sqrt{3}(v_3 - v_0) + a(\psi_3 + \psi_0)\right) \tag{46}$$

$$M_{30} = \frac{EI}{a}\left(\psi_3 - \psi_0\right),$$

In this analysis it is necessary to eliminate the displacements and rotation at the joint 0 to obtain representations of the displacements and rotations of the position vectors b_1 and b_2. To accomplish this, we invert the force-displacement relations to get the displacement-force relations. For beam 10, these become

$$(u_1 - u_0) = \frac{a^2}{12EI}\left(aT_{10} - 6M_{10}\right) - a\psi_0$$

$$(v_1 - v_0) = \frac{a}{EA}P_{10} \tag{47}$$

$$(\psi_1 - \psi_0) = \frac{a}{EI}M_{10},$$

and for beams 20 and 30 we get

$$(u_2 - u_0) = \frac{a\sqrt{3}}{2EA}P_{20} - \frac{a^2}{24EI}\left(aT_{20} - 6M_{20}\right) + \frac{a}{2}\psi_0$$

$$(v_2 - v_0) = -\frac{a}{2EA}P_{20} - \frac{a^2\sqrt{3}}{24EI}\left(aT_{20} - 6M_{20}\right) + \frac{a\sqrt{3}}{2}\psi_0 \tag{48}$$

$$(\psi_2 - \psi_0) = \frac{a}{EI}M_{20},$$

and

$$(u_3 - u_0) = -\frac{a\sqrt{3}}{2EA}P_{30} - \frac{a^2}{24EI}\left(aT_{30} - 6M_{30}\right) + \frac{a}{2}\psi_0$$

$$(v_3 - v_0) = -\frac{a}{2EA}P_{30} + \frac{a^2\sqrt{3}}{24EI}\left(aT_{30} - 6M_{30}\right) - \frac{a\sqrt{3}}{2}\psi_0 \tag{49}$$

$$(\psi_3 - \psi_0) = \frac{a}{EI}M_{30}.$$

To relate these displacements and rotations to the joint 3 we observe that

$$\left.\begin{aligned}
(u_i - u_3) &= (u_i - u_0) - (u_3 - u_0) \\
(v_i - v_3) &= (v_i - v_0) - (v_3 - v_0) \\
(\psi_i - \psi_3) &= (\psi_i - \psi_0) - (\psi_3 - \psi_0)
\end{aligned}\right\} \quad \text{for } i = (1,2). \tag{50}$$

Substituting (47), (48), and (49) into (50) provides the six relations

$$(u_1 - u_3)$$
$$= +\frac{a\sqrt{3}}{2EA}P_{30} + \frac{a^2}{24EI}\left(2aT_{10} + aT_{30} - 12M_{10} + 30M_{30}\right) - \frac{3a}{2}\psi_3$$

$$(v_1 - v_3)$$
$$= +\frac{a}{2EA}\left(2P_{10} + P_{30}\right) - \frac{a^2\sqrt{3}}{24EI}\left(aT_{30} + 6M_{30}\right) + \frac{a\sqrt{3}}{2}\psi_3$$

$$(\psi_1 - \psi_2) = \frac{a}{EI}\left(M_{10} - M_{30}\right)$$

$$(u_2 - u_3)$$
$$= \frac{a\sqrt{3}}{2EA}\left(P_{20} + P_{30}\right) - \frac{a^2}{24EI}\left(aT_{20} - aT_{30} - 6M_{20} + 6M_{30}\right)$$

$$(v_2 - v_3)$$
$$= -\frac{a}{2EA}\left(P_{20} - P_{30}\right) - \frac{a^2\sqrt{3}}{24EI}\left(aT_{20} + aT_{30} - 6M_{20} + 18M_{30}\right) + a\sqrt{3}\psi_3$$

$$(\psi_2 - \psi_3) = \frac{a}{EI}\left(M_{20} - M_{30}\right). \tag{51}$$

Equilibrium of the fundamental element requires

$$\begin{aligned}
2T_{10} - T_{20} - T_{30} + \sqrt{3}(P_{20} - P_{30}) &= 0 \\
2P_{10} - P_{20} - P_{30} - \sqrt{3}(T_{20} - T_{30}) &= 0 \\
2(M_{10} + M_{20} + M_{30}) - a(T_{10} + T_{20} + T_{30}) &= 0.
\end{aligned} \tag{52}$$

The nine equations of (51) and (52) are sufficient to determine the six forces and three midpoint moments of the three beams in terms of the displacements and rotations of the joints 1,2, and 3. As in the triangular structure, we introduce the beam stretching and bending compliances M and N given by (25). From (51) and (52), the axial and transverse forces and midpoint moment

in beam 01 are given by

$$12\sqrt{3}M(M+N)P_{10} = (3M+N)\sqrt{3}\big(2(v_1-v_3)-(v_2-v_3)\big)$$
$$-3(M-N)(u_2-u_3)+3Ma(\psi_2-\psi_3),$$

$$\text{(53)}$$

$$48N(M+N)T_{10} = 6a(M+N)\psi_3$$
$$+(M+N)\big(2(u_1-u_3)-(u_2-u_3)-\sqrt{3}(v_2-v_3)\big)$$
$$+8N\big(2(u_1-u_3)-(u_2-u_3)+\sqrt{3}(v_2-v_3)\big)$$
$$+2a(M+5N)(\psi_1-\psi_3)+2a(M-N)(\psi_2-\psi_3),$$

$$\text{(54)}$$

and

$$96NM_{10} = a\bigg\{\big[2(u_1-u_3)-(u_2-u_3)-\sqrt{3}(v_2-v_3)\big]$$
$$+6a\psi_3+\frac{14a}{3}(\psi_1-\psi_3)+\frac{2a}{3}(\psi_2-\psi_3)\bigg\}.$$

$$\text{(55)}$$

Similar expressions may be obtained for the forces and moments in beams 02 and 03.

To effect a continuum representation of this structure, we again assume the existence of continuous displacement fields $u(x,y)$ and $v(x,y)$, and a continuous rotation field $\psi(x,y)$ such that the displacements and rotations of joints 1 and 2 can be expressed as Taylor series about the joint 3. This provides

$$(u_1-u_3) = \frac{a\sqrt{3}}{2}\left(\frac{\partial u}{\partial x}+\sqrt{3}\frac{\partial u}{\partial y}\right)+\frac{3a^2}{8}\left(\frac{\partial^2 u}{\partial x^2}+2\sqrt{3}\frac{\partial^2 u}{\partial x\partial y}+3\frac{\partial^2 u}{\partial y^2}\right)$$

$$(v_1-v_3) = \frac{a\sqrt{3}}{2}\left(\frac{\partial v}{\partial x}+\sqrt{3}\frac{\partial v}{\partial y}\right)+\frac{3a^2}{8}\left(\frac{\partial^2 v}{\partial x^2}+2\sqrt{3}\frac{\partial^2 v}{\partial x\partial y}+3\frac{\partial^2 v}{\partial y^2}\right)$$

$$(\psi_1-\psi_3) = \frac{a\sqrt{3}}{2}\left(\frac{\partial \psi}{\partial x}+\sqrt{3}\frac{\partial \psi}{\partial y}\right)+\frac{3a^2}{8}\left(\frac{\partial^2 \psi}{\partial x^2}+2\sqrt{3}\frac{\partial^2 \psi}{\partial x\partial y}+3\frac{\partial^2 \psi}{\partial y^2}\right)$$

$$(u_2-u_3) = a\sqrt{3}\frac{\partial u}{\partial x}+\frac{3a^2}{2}\frac{\partial^2 u}{\partial x^2}$$

$$(v_2-v_3) = a\sqrt{3}\frac{\partial v}{\partial x}+\frac{3a^2}{2}\frac{\partial^2 v}{\partial x^2}$$

$$(\psi_2-\psi_3) = a\sqrt{3}\frac{\partial \psi}{\partial x}+\frac{3a^2}{2}\frac{\partial^2 \psi}{\partial x^2},$$

$$\text{(56)}$$

where we have retained terms of order a^2 and all derivatives are evaluated at point 3. With the displacements and rotations expressed by (56), the beam

forces and moment in beam 10 are given by

$$P_{10} = \frac{a}{4M(M+N)} \left\{ (3M+N)\frac{\partial v}{\partial y} - (M-N)\frac{\partial u}{\partial x} \right\}$$

$$T_{10} = \frac{a}{16N(M+N)} \left\{ (M+N)\left(2\psi + \frac{\partial u}{\partial y} - \frac{\partial v}{\partial x}\right) \right.$$
$$\left. +8N\left(\frac{\partial u}{\partial y} + \frac{\partial v}{\partial x}\right) \right\} \tag{57}$$

$$M_{10} = \frac{a^2}{32N} \left\{ \left(2\psi + \frac{\partial u}{\partial y} - \frac{\partial v}{\partial x}\right) + \frac{10a}{3}\frac{\partial \psi}{\partial y} \right\},$$

where the terms in (57) are now evaluated at joint 0 of Fig. 7. The forces and midpoint moments in beams 20 and 30 are represented in a similar way.
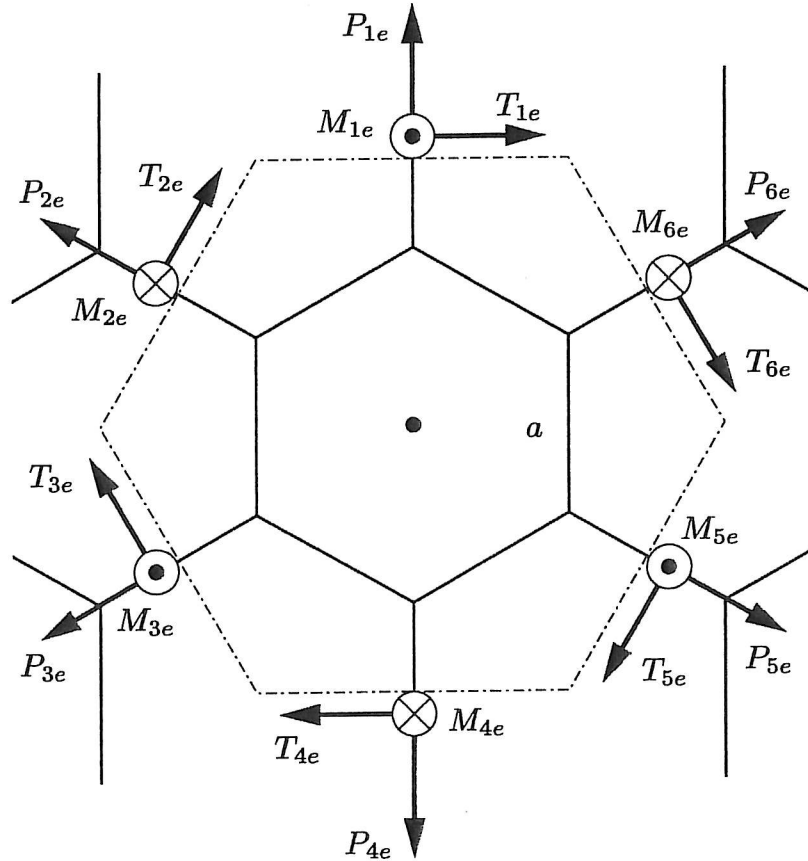

Fig. 9. Representative volume element for the honeycomb structure with resultant forces and moments on the six faces.

The representative volume element of Fig. 7 is shown in more detail in Fig. 9 where we have relabeled the joints as shown. Note that the sides of

this element pass through the beam midpoints. The forces and moments in the 3 beams associated with the joint 0 are known explicitly in a form similar to that of (57). The forces and moments in the remaining beams within the representative element are obtained from Taylor series expansions about the joint 0 of these three known forces. These expansions are consistent with our assumption that the displacement and rotation fields are differentiable as often as necessary. For example, the forces and moments in the three beams 12, 22, and 32 associated with joint 2 of Fig. 7, located at the point $(-a\sqrt{3}/2, -3a/2)$ with respect to the joint 0, are denoted by P_{12}, T_{12}, M_{12}, P_{22} etc. and are given by

$$
\begin{aligned}
P_{12} &= P_{10} - \frac{a\sqrt{3}}{2}\frac{\partial P_{10}}{\partial x} - \frac{3a}{2}\frac{\partial P_{10}}{\partial y} + \cdots \\[2mm]
T_{12} &= T_{10} - \frac{a\sqrt{3}}{2}\frac{\partial T_{10}}{\partial x} - \frac{3a}{2}\frac{\partial T_{10}}{\partial y} + \cdots \\[2mm]
M_{12} &= M_{10} - \frac{a\sqrt{3}}{2}\frac{\partial M_{10}}{\partial x} - \frac{3a}{2}\frac{\partial M_{10}}{\partial y} + \cdots
\end{aligned}
\tag{58}
$$

with similar expressions for the forces and moments in beams 22 and 32. In these expressions, all variables are evaluated at the center of the element $(0, -a)$ with respect to the point 0 of Fig. 7. This procedure determines all forces and moments in the beams of the representative volume element in terms of the displacement and rotation fields.

5.2 Effective Stresses

Estimates of the effective stresses and couple stresses may be determined by many different methods. Here, we have chosen to do it by volume averaging of the forces and moments acting on the boundary of the representative volume element. The volume averaged stresses $\bar{\sigma}_{\alpha\beta}$ are then given by

$$
V\bar{\sigma}_{\alpha\beta} = \sum_{n=1}^{N} x_{\alpha}^{n} F_{\beta}^{n}
\tag{59}
$$

where $V = a^2 9\sqrt{3}/2$ is the area of the representative volume element.

Using (59), the stresses become

$$\bar{\sigma}_{xx} = \frac{1}{4\sqrt{3}M}L_1 + \frac{1}{2\sqrt{3}(M+N)}L_2$$

$$\bar{\sigma}_{yy} = \frac{1}{4\sqrt{3}M}L_1 - \frac{1}{2\sqrt{3}(M+N)}L_2 \qquad (60)$$

$$(\bar{\sigma}_{xy} + \bar{\sigma}_{yx}) = \frac{1}{\sqrt{3}(M+N)}L_3$$

and by

$$(\bar{\sigma}_{xy} - \bar{\sigma}_{yx}) = \frac{1}{8\sqrt{3}N}\left[L_4 - \frac{a^2}{4}\nabla^2\psi\right] \qquad (61)$$

We note that the term $\nabla^2\psi$ occurring in (61) is isotropic and thus satisfies the three-fold symmetry condition. The moment equilibrium equation (26) provides a second representation for the shear stress difference in the form

$$(\bar{\sigma}_{xy} - \bar{\sigma}_{yx}) = -\frac{a^2}{24\sqrt{3}N}\left[\nabla^2\psi + \tfrac{3}{8}\nabla^2 L_4\right] \qquad (62)$$

which shows that the shear stress difference $(\bar{\sigma}_{xy} - \bar{\sigma}_{yx})$ and the shear strain difference L_4 are both of order a^2. Furthermore, L_4 and ψ satisfy the relation

$$L_4 + \frac{a^2}{12}\nabla^2\psi = 0 \qquad (63)$$

where we have suppressed terms of order a^4. Using (63), the shear stress difference is given by

$$(\bar{\sigma}_{xy} - \bar{\sigma}_{yx}) = \frac{1}{2\sqrt{3}N}L_4 \qquad (64)$$

The couple stresses are estimated by volume averaging as given by (35) which provides

$$\bar{\mu}_{xz} = \frac{a^2}{24\sqrt{3}N}\left[\frac{\partial\psi}{\partial x} + \frac{3}{8}\frac{\partial L_4}{\partial x}\right] + O(a^3)$$

$$\bar{\mu}_{yz} = \frac{a^2}{24\sqrt{3}N}\left[\frac{\partial\psi}{\partial y} + \frac{3}{8}\frac{\partial L_4}{\partial y}\right] + O(a^3) \qquad (65)$$

The relations of (60), (64) and (65) provide the constitutive relations for the honeycomb structure which satisfy the three-fold symmetry conditions. For this honeycomb structure, the non-zero coefficients a_i of (12) are

$$a_1 = \frac{1}{4\sqrt{3}M}, \quad a_2 = \frac{1}{2\sqrt{3}(M+N)}, \quad a_6 = \frac{1}{4\sqrt{3}N} \qquad (66)$$

and the non-zero b_i of (12) are

$$b_1 = \frac{a^2}{24\sqrt{3}N} \;, \quad b_7 = \frac{a^2}{64\sqrt{3}N} \tag{67}$$

5.3   Example—Simple Bending

Also for the honeycomb material we analyze the simple bending deformation defined by Fig. 6. Here,

$$u = -kyx \;, \quad v = \frac{1}{2}k\left[x^2 + \frac{(N-M)}{(3M+N)}y^2\right] \;, \quad \psi = kx \tag{68}$$

where k is the curvature of the bent material. The quantities

$$L_1 = -\frac{4M}{(3M+N)}ky \;, \quad L_2 = -\frac{2(M+N)}{(3M+N)}ky \;, \quad L_3 = 0 \;, \quad L_4 = 0 \tag{69}$$

provide the stresses

$$\bar{\sigma}_{xx} = -\frac{2}{\sqrt{3}(3M+N)}ky \;, \quad \bar{\sigma}_{xy} = \bar{\sigma}_{yx} = \bar{\sigma}_{yy} = 0 \;, \tag{70}$$

and the couple stresses

$$\bar{\mu}_{xz} = \frac{a^2}{24\sqrt{3}N}k \;, \quad \bar{\mu}_{yz} = 0 \tag{71}$$

Again, as the strut length $a \to 0$ the micropolar effect vanishes and the rotation ψ becomes equal to the local infinitesimal rigid rotation.

This stress and displacement field is again representative of the response of a rectangular beam of depth h, width b, and length l bent with uniform curvature k. Here, the moment $\mathcal{M}$ which must be applied at the ends of the beam to support this deformation is given by

$$\mathcal{M} = \frac{kbh^3}{6\sqrt{3}(3M+N)}\left[1 + \frac{(3M+N)}{4N}\left(\frac{a}{h}\right)^2\right] \tag{72}$$

Again, for $N \gg M$, the moment $\mathcal{M}$ becomes

$$\mathcal{M} = \frac{kbh^3}{6\sqrt{3}N}\left[1 + \frac{1}{4}\left(\frac{a}{h}\right)^2\right] \tag{73}$$

Comparison with (43) for the equilateral triangle structure shows that the moment required to bend the equilateral triangle structure through the curvature k is significantly greater than for the hexagonal structure.

6 Comparison with Other Work

In a recent micropolar analysis of both the equilateral triangle and the honeycomb structures, Chen et al. (1998) develop expressions for the strain energy density of the structure as a superposition of the strain energies of the individual struts. This leads them to the erroneous conclusion that the strain energy density of the equilateral triangle structure is three times that of the honeycomb because the equilateral triangle structure contains three times as many struts per unit volume at each orientation as the honeycomb. This approach ignores the actual connectivity of the individual structures and also equilibrium conditions at the joints.

	a_1	a_2	a_6	b_1
Present	$\dfrac{\sqrt{3}}{4M}$	$\dfrac{\sqrt{3}(M+N)}{8MN}$	$\dfrac{\sqrt{3}}{4N}$	$\dfrac{a^2\sqrt{3}}{24N}$
Chen et al.	$\dfrac{\sqrt{3}}{4M}$	$\dfrac{\sqrt{3}(M+N)}{8MN}$	$\dfrac{\sqrt{3}}{4N}$	$\dfrac{a^2\sqrt{3}}{6N}$

Table 1. Results for the equilateral triangle structure.

While their results for the stresses in the triangle structure agree with ours, see Table 1, their constitutive relation for the honeycomb predicts a much too stiff behavior, see Table 2. This is also demonstrated by our results for the two simple bending deformations of (43) and (73). In general any deformation pattern dominated by bending of the beams is predicted to require loads that are much too great. Also, for homogeneous deformations, their results do not agree with those of Warren & Kraynik (1987). For both structures the couple stresses obtained by Chen et al. (1998) are four times those obtained here, see Tables 1 and 2. The source of this difference is not clear but may be related to their definition of the strain tensor. It appears that their strain tensor is symmetric but they also introduce an independent rotation θ which is not accounted for in their definition of the strain tensor. In fact, the quantity $(\theta - \omega) = \frac{1}{2}(\varepsilon_{yx} - \varepsilon_{xy})$, and if the strain tensor is symmetric, $\theta = \omega$ and is not an independent rotation. Chen et al. (1998) then go on and utilize their constitutive relations to investigate the fracture toughness of these reticulated materials.

	a_1	a_2	a_6	b_1	b_7
Present	$\dfrac{1}{4\sqrt{3}M}$	$\dfrac{1}{2\sqrt{3}(M+N)}$	$\dfrac{1}{4\sqrt{3}N}$	$\dfrac{a^2}{24\sqrt{3}N}$	$\dfrac{a^2}{64\sqrt{3}N}$
W & S	$\dfrac{1}{4\sqrt{3}M}$	$\dfrac{1}{2\sqrt{3}(M+N)}$	$\dfrac{1}{4\sqrt{3}N}$	$\dfrac{a^2}{24\sqrt{3}N}$	0
Chen et al.	$\dfrac{1}{4\sqrt{3}M}$	$\dfrac{(N+M)}{8\sqrt{3}MN}$	$\dfrac{1}{4\sqrt{3}N}$	$\dfrac{a^2}{6\sqrt{3}N}$	0

Table 2. Results for the honeycomb structure.

Wang & Stronge (1999) have provided an analysis of the micropolar behavior of the honeycomb structure. They utilize a novel representative volume element and obtain the stresses and couple stresses from equilibrium conditions enforced on the element. They also enforce the three-fold symmetry condition and account for equilibrium at the joints and connectivity of the structure. Their constitutive equations agree with those presented here, see Table 2. Their constitutive equations for the couple stresses assume only a non-zero b_1 which is consistent with our results in that the term involving b_7 is actually of order a^4 and should therefore be ignored for consistency. They use their constitutive equations to solve an interesting contact problem on the half-plane.

7   Discussion

In the classical couple stress and micropolar theories, a characteristic length appears which is assumed to be an intrinsic material property. One of the major problems involved in relating these theories to observed material behavior is the determination of this characteristic length. In general, most heterogeneous materials will exhibit a number of length scales depending on the composition of the particular material under investigation. This has stimulated an interest in the mechanical properties of random structures characterized by a fractal dimension (Limat 1988b). The approach utilizes the theory of micropolar elasticity within the framework of lattice percolation theory. In this theory, the material is generally modeled as a two-dimensional lattice of rigid particles which undergo motions of both translation and rotation, and are connected by elastic ligaments of random rigidity. Each ligament is assumed to deform independently. The mechanical response of this lattice structure is represented

in the form of an elastic strain energy density function taken as the sum of the strain energy of each ligament, and involves the strains and rotations within the lattice in a form characteristic of micropolar materials. Connectivity of the lattice and equilibrium of the forces and moments induced on the rigid particles by the elastic ligaments is generally not considered in these models.

Ignoring the specific connectivity of the structure can have significant effects on estimates of the elastic constants. This has been pointed out by Warren & Kraynik (1997) and by Zhu, Knott & Mills (1997) in their investigations of the mechanical response of the three-dimensional spatially periodic connected tetrakaidecohedron. They show that the effective elastic constants for this connected structure are approximately 30 percent less than those for a random array of tetrahedral joints (Warren & Kraynik 1988). They also point out that torsion effects of the struts is significant for distortion type deformations.

In this investigation of micropolar effects in spatially periodic structures, the characteristic length is well defined as the intrinsic beam length a associated with the geometry of the structure. We have shown that in the transition from the discrete structure to the continuum model representative of the material's mechanical response, it is necessary to carry terms through second order in a in the Taylor series representations of the displacements and rotations of the material points. In their analysis, Askar & Cakmak (1968) retain only first order terms and we have shown that this does not provide a micropolar continuum. The necessity of carrying the second order terms to investigate micropolar effects has been pointed out previously by Bažant & Christensen (1972), who suppress a number of strain gradient terms in the constitutive relations they develop which we feel should be included for consistency. Typically in most micropolar work, and also in the couple stress theory, the only second gradients of displacements considered are the infinitesimal rotation gradients. We see no a priori justification for suppressing all other strain gradients. In the limit as $a \to 0$ the continuum model reduces to that of a simple hyperelastic material.

The mechanical response of low-density solid foams has been studied using micromechanical models of a spatially periodic structure (Warren & Kraynik 1987, Warren & Kraynik 1988). These models assume a homogeneous deformation of the structure and show how the elastic response depends on specific aspects of the cell morphology and microstructure. Under these conditions, the elastic response is not micropolar. These low-density foams are often used for shock and vibration mitigation, and in these applications are often loaded beyond the elastic limit and crushed. At the present time there is no adequate micromechanical model which characterizes this generally inelastic and non-recoverable deformation. Experimental evidence indicates that this crushing or buckling of the foam is highly localized (Klintworth & Stronge 1989, Papka & Kyriakides 1994), occurring along thin bands running through the structure. Thus this crushing or buckling of the structure represents a deformation of the structure which is not homogeneous but highly localized, and the contin-

uum model of this crushing may be representative of a micropolar material as suggested by the work of Bažant & Christensen (1972). The linear elastic micropolar model developed here cannot be used to investigate localized deformations to failure when these deformations become large. Micropolar effects, however, may provide information on where and under what conditions eventual failure modes initiate. To actually obtain failure patterns for a given loading orientation, the nonlinear material behavior for the specific material used to fabricate the reticulated structure must be characterized as done by Papka & Kyriakides (1998). But since actual nonlinear material behavior is very diverse, these large deformation analyses become material specific and loose their generality. The present analysis may also be useful for investigating the properties of polydisperse cellular structures and indicate under what conditions the structure resembles a micropolar continuum.

8   Acknowledgement

References

Askar, A. & Cakmak, A. S. (1968). A structural model of a micropolar continuum, *Int. J. Engng. Sci.* **6**: 583–589.

Bažant, Z. P. (1971). Micropolar medium as a model for buckling of grid frameworks, *Proc. 12th Midwestern Mech. Conf.*, Vol. 6, pp. 587–594.

Bažant, Z. P. & Christensen, M. (1972). Analogy between micropolar continuum and grid frameworks under initial stress, *Int. J. Solids Struct.* **8**: 327–346.

Chen, J. Y., Huang, Y. & Ortiz, M. (1998). Fracture analysis of cellular materials: A strain gradient model, *J. Mech. Phys. Solids* **46**(5): 789–828.

Christensen, R. (1987). Sufficient symmetry conditions for isotropy of the elastic muduli tensor, *J. App. Mech.* **54**(4): 772–777.

Christoffersen, J. (1996). Material curvature. Unpublished note on Nonlinear Micropolar Theories.

Eringen, A. C. (1966). Linear theory of micropolar elasticity, *J. Math. Mech.* **15**: 909–923.

Eringen, A. C. & Suhubi, E. S. (1964). Nonlinear theory of simple micro-elastic solids-I, *Int. J. Engng. Sci.* **2**: 189–203.

Feng, S. (1985). Percolation properties of granular elastic networks in two dimensions, *Phys. Rev. B* **32**: 510–513.

Klintworth, J. W. & Stronge, W. J. (1989). Plane punch indentation of a ductile honeycomb, *Int. J. Mech. Sci.* **31**: 359–378.

Koiter, W. T. (1964). Couple stresses in the theory of elasticity, I and II, *Proc. Ned. Acad. Wet. (B)*, Vol. 67, pp. 17–44.

Limat, L. (1988a). Micropolar elastic percolation: The superelastic problem, *Phys. Rev. B* **38**: 7219–7222.

Limat, L. (1988b). Percolation and cosserat elasticity: Exact results on a deterministic fractal, *Phys. Rev. B* **37**: 672–675.

Mindlin, R. D. (1968). Theories of elastic continua and lattice theories, *in* E. Kröner (ed.), *Proc. 1967 IUTAM Symposium on Generalized Continua*, Springer-Verlag, New York, pp. 312–320.

Nemat-Nasser, S. & Hori, M. (1993). *Micromechanics: Overall Properties of Heterogeneous Materials*, North-Holland, Amsterdam.

Papka, S. D. & Kyriakides, S. (1994). In-plane compressive response and crushing of honeycomb, *J. Mech. Phys. Solids* **42**(10): 1499–1532.

Papka, S. D. & Kyriakides, S. (1998). In-plane crushing of a polycarbonate honeycomb, *Int. J. Solids Struct.* **42**(10): 1499–1532.

Sun, C. T. & Yang, T. Y. (1973). A contiuum approach toward dynamics of gridworks, *J. Appl. Mech.* **40**: 186–192.

Wang, X. L. & Stronge, W. (1999). Micropolar theory for two-dimensional stresses in elastic honeycomb, *Proc. Roy. Soc., A* **455**: 2091–2116.

Warren, W. E. & Kraynik, A. M. (1987). Foam mechanics: The linear elastic response of two-dimensional spatially periodic cellular materials, *Mech. Mat.* **6**: 27–37.

Warren, W. E. & Kraynik, A. M. (1988). The linear elastic properties of open-cell foams, *J. Appl. Mech.* **110**: 341–346.

Warren, W. E. & Kraynik, A. M. (1997). Linear elastic behavior of a low-density kelvin foam with open cells, *J. Appl. Mech.* **64**(4): 787–794.

Zhu, H. X., Knott, J. F. & Mills, N. J. (1997). Analysis of the elastic properties of open-cell foams with tetrakaidicahedral cells, *J. Mech. Phys. Solids.* **45**(3): 319–343.
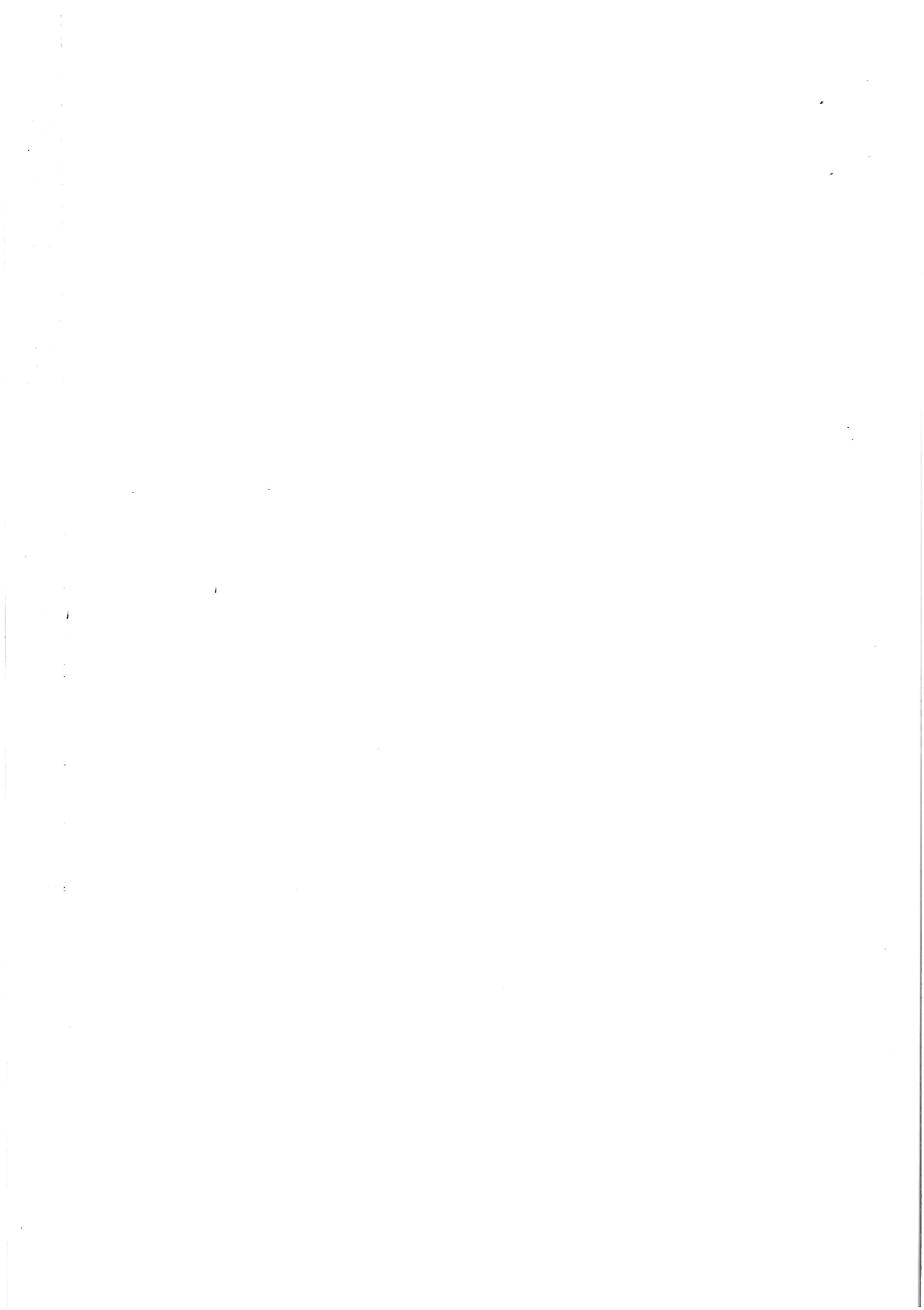
RECENT PAPERS ON STRUCTURAL AND SOLID MECHANICS

PAPER NO. 1: W.E. Warren, E. Byskov: *Three-Fold Symmetry Restrictions on Two-Dimensional Micropolar Materials*. ISSN 1395-7953 R0053.

PAPER NO. 2: L. Pilgaard Mikkelsen: *Necking of Stretched Sheets Modelled by a 2-D Nonlocal Plasticity Model*. ISSN 1395-7953 R0054.

PAPER NO. 3: : L. Pilgaard Mikkelsen: *A Numerical Elastic-Viscoplastic Collapse Analysis of Circular Cylindrical Shells under Axial Compression*. ISSN 1395-7953 R0055.

Complete list of papers: http://www.civil.auc.dk/i6/publ/ssmech.html